Electronic Supplementary Material (ESI) for Physical Chemistry Chemical Physics.

SUPPORTING INFORMATION

Tuning Core-Shell Interactions in Tungsten Carbide-Pt Nanoparticles for the Hydrogen Evolution Reaction

Akash Jain[1] **and Ashwin Ramasubramaniam**[2,*]

[1] Department of Chemical Engineering, University of Massachusetts, Amherst, MA 01003, U.S.A.

[2] Department of Mechanical and Industrial Engineering, University of Massachusetts, Amherst, MA 01003, U.S.A.

*E-mail: ashwin@engin.umass.edu

1. Surface energy calculations

For stochiometric surfaces of WC, the surface energy (γ) is defined as,

$$\gamma_{surface} = \frac{E_{Slab} - N_{WC}\,\mu_{WC\,(Bulk)}}{A_0}, \quad \text{(S1)}$$

where E_{Slab} is the energy of periodic and symmetric surface slab, $\mu_{WC\ (Bulk)}$ is the chemical potential of bulk α-WC or β-WC per WC pair, N_{WC} is the total number of WC pairs in the slab, and A_0 is total surface area of the slab.

For non-stochiometric surfaces, the surface energy (γ) is defined as,[1,2]

$$\gamma_{surface} = \frac{E_{Slab} - N_W\,\mu_W - N_C\,\mu_C}{A_0}, \quad \text{(S2)}$$

$$\mu_{WC(Bulk)} = \mu_W + \mu_C, \quad \text{(S3)}$$

$$\mu_{C,graphene} + \Delta H_{f,\alpha/\beta-WC} < \mu_C < \mu_{C,graphene}, \quad \text{(S4)}$$

where μ_W and μ_C are the chemical potentials of bulk bcc W and C (graphene) respectively, N_W and N_C are the number of W and C atoms in the slab, and A_0 is total surface area of the slab.

Figure S1 reports surface energies for various WC surfaces and is in good agreement with preior results of Li *et al.* [3] and Yates *et al.*[4]

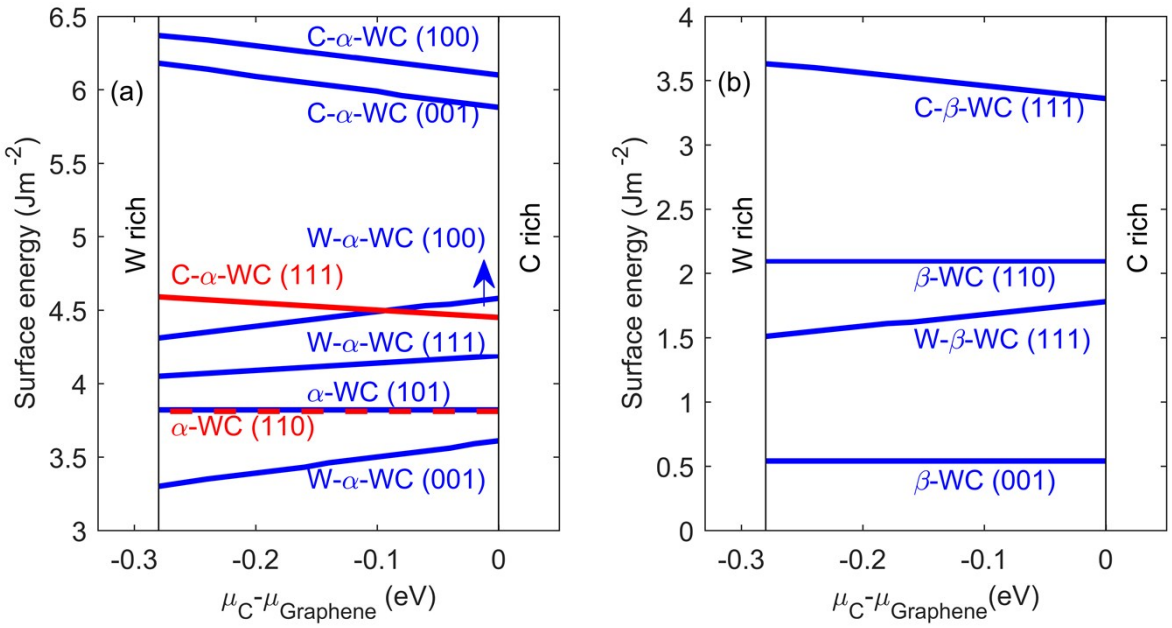

Figure S1. Surface energies of select low Miller-index surfaces of (a) α-WC and (b) β-WC as a function of chemical potential of carbon (relative to graphene)

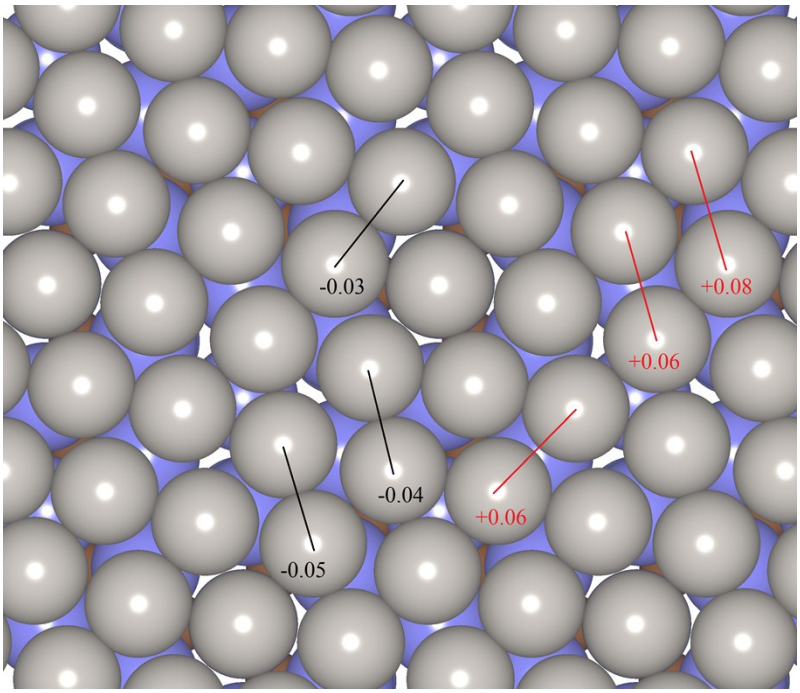

Figure S2. Relaxed structure of Pt ML over α-WC (001) support in the p-(4x4) R15° supercell. W and Pt atoms are indicated by blue and grey spheres, respectively; C atoms are not visible in this view. The relaxed Pt ML has regions of both compressive and tensile strain; bond strains, $\varepsilon_b = a/a_{Pt(111)}-1$ ($a_{Pt(111)}$=2.81 Å), are indicated at a few sites.

2. DFT-based *ab initio* molecular dynamics (AIMD)

To test the stability of Pt monolayers over β-WC (111) and β-WC (001) surfaces, Pt_{ML}/β-WC (111) and Pt_{ML}/β-WC (001) slabs were subjected to DFT-based *ab initio* molecular dynamics (AIMD) at elevated temperatures. The system was heated from 0 to 1000 K at a rate of 2 K/fs over a duration of 0.5ps and then held at 1000K for another 0.5ps in a canonical ensemble. The monolayers retain their structural integrity over this entire process (Figures S3 & S4).

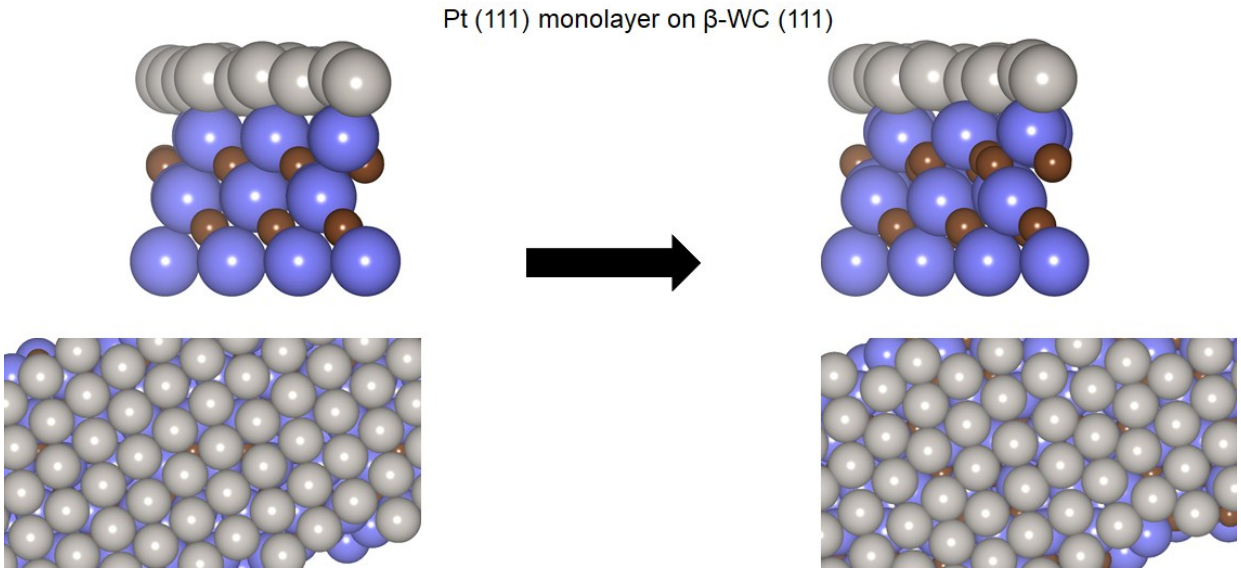

Figure S3. Pt_{ML}/β-WC (111) before (left) and after (right) AIMD trajectory

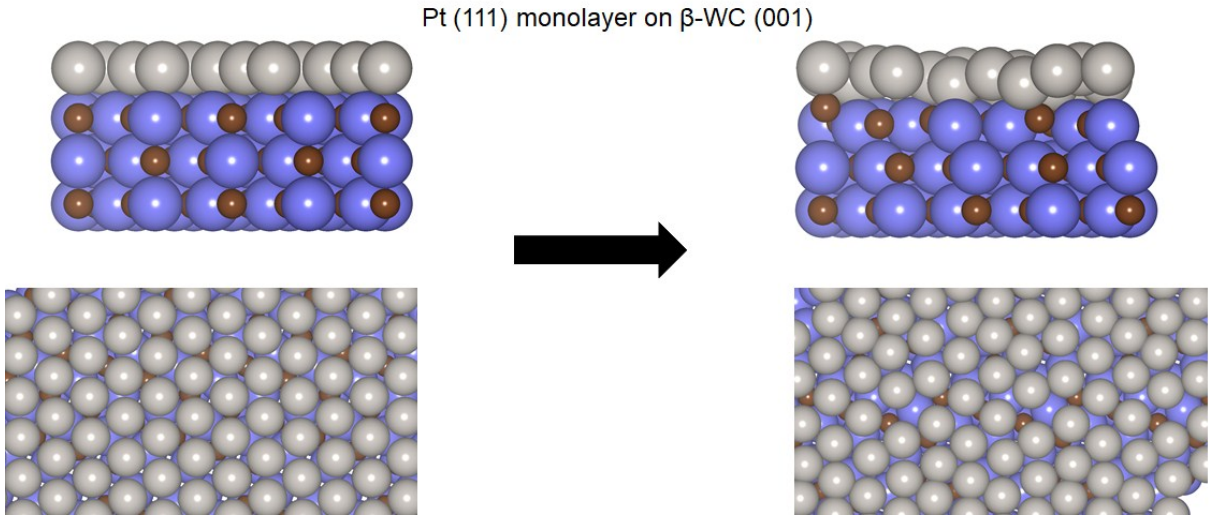

Figure S4. Pt_{ML}/β-WC (001) before (left) and after (right) AIMD trajectory

3. Preferred location of Ti atoms in β-WC (111) and Pt_{ML} /β-WC (111) slabs

To determine the preferred sites for Ti atoms in β-WC (111) and Pt_{ML} /β-WC (111) slabs (shown in Figures S6 & S7), we calculated the heat of formation, E_f, of the slabs with a single Ti dopant atom in different W layers of the slab; the three bottommost layers (2 C and 1 W) were frozen to simulate bulk-like conditions while the remaining layers were subjected to structural relaxation. The heat of formation is defined as

$$E_f = \frac{E_{Slab} - n_W \mu_W - n_C \mu_C - n_{Pt} \mu_{Pt} - \mu_{Ti}}{V}, \quad \text{(S5)}$$

where E_{Slab} is the total energy of slab; μ_W, μ_C, μ_{Pt} and μ_{Ti} are the chemical potentials of bulk W, C (graphene), Pt and Ti; n_W, n_C, n_{Pt} are the number of W, C and Pt atoms in the slab; and V is volume of the slab. As seen from Figures S6 & S7, there is a slight preference for the Ti

atom to occupy the second W subsurface layer; the energy differences are small enough though that the alloy such segregation effects may be neglected in the DFT model.

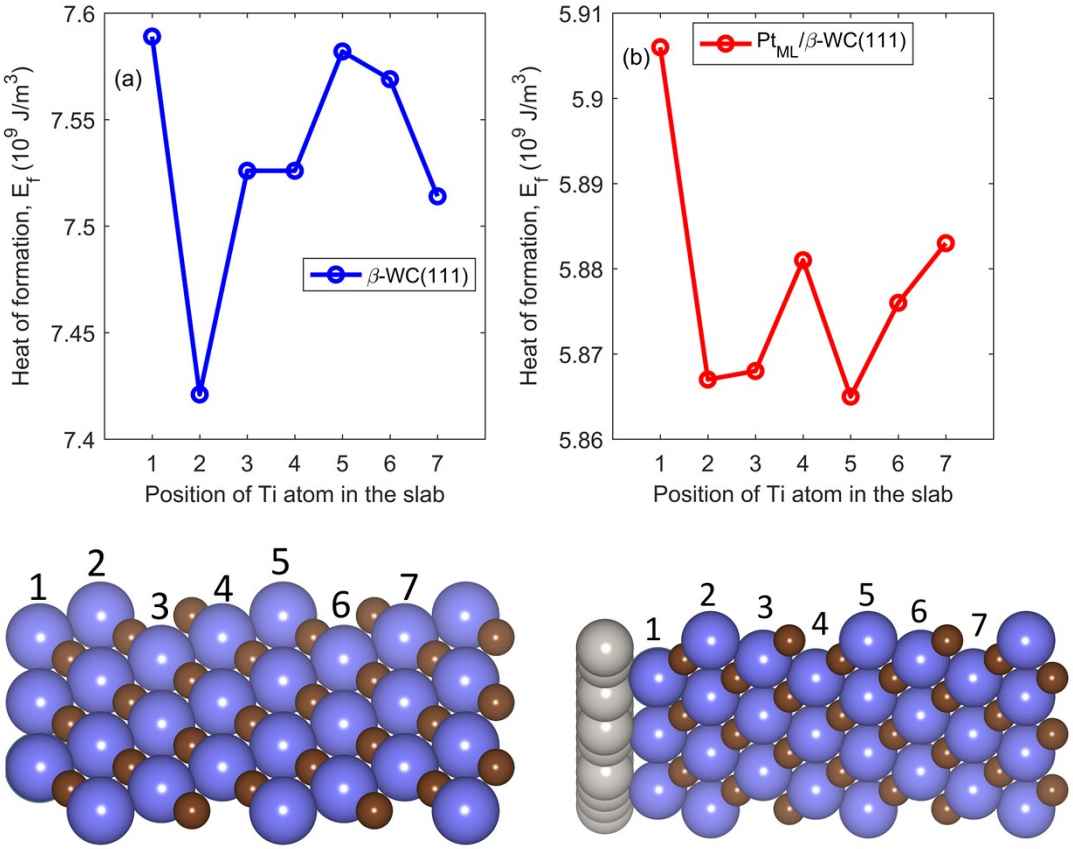

Figure S5. Heat of formation of (a) β-WC (111) and (b) Pt_{ML}/β-WC (111) slabs as function of the position of a single Ti dopant atom (W – large blue spheres; C – small, brown spheres; Pt- large grey spheres)

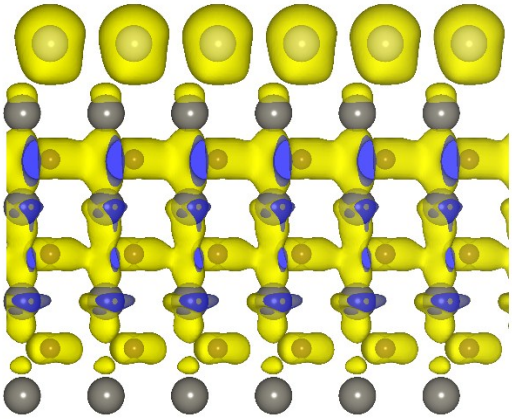

Figure S6. Partial charge density of Pt_{ML}/α-WC (001) within an energy window of ± 0.2 eV of the Fermi level; isosurfaces are plotted at a value of 0.007 e/Å^3

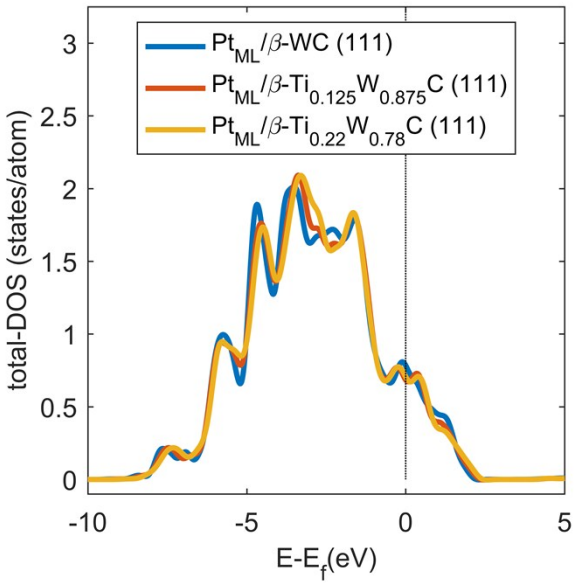

Figure S7. Total density of states for various Pt_{ML}/β-$Ti_xW_{1-x}C$ (111) systems studied

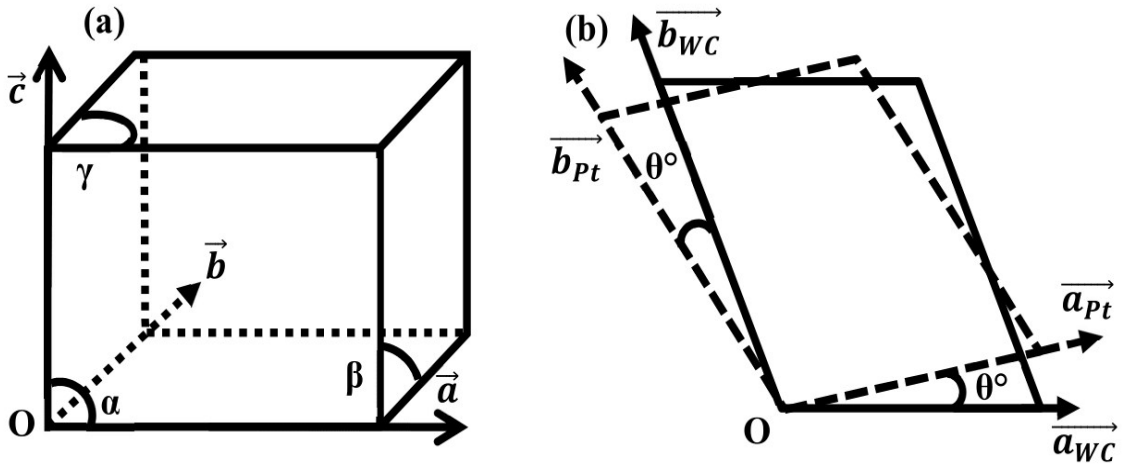

Figure S8. (a) Schematic of the supercell for the WC surface slabs and (b) illustration of the Pt (111) ML being rotated by an angle θ° with respect to WC surface supercell

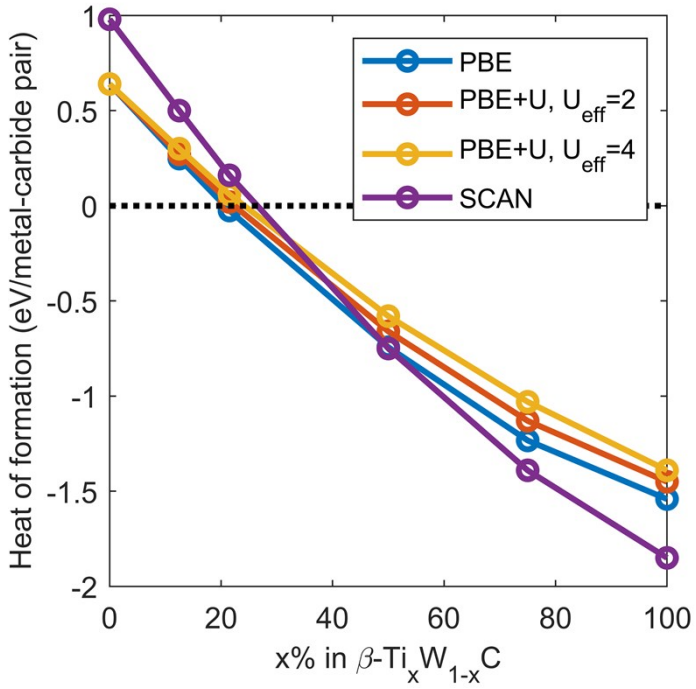

Figure S9. Heat of formation of β-$Ti_xW_{1-x}C$ alloy (Eq. 7 in manuscript) as a function of Ti content (*x*%) with PBE, PBE+U, and SCAN functionals; two different values of U_{eff}=U-J are employed here for comparison. All calculations are performed at PBE-optimized lattice parameters and atomic positions.

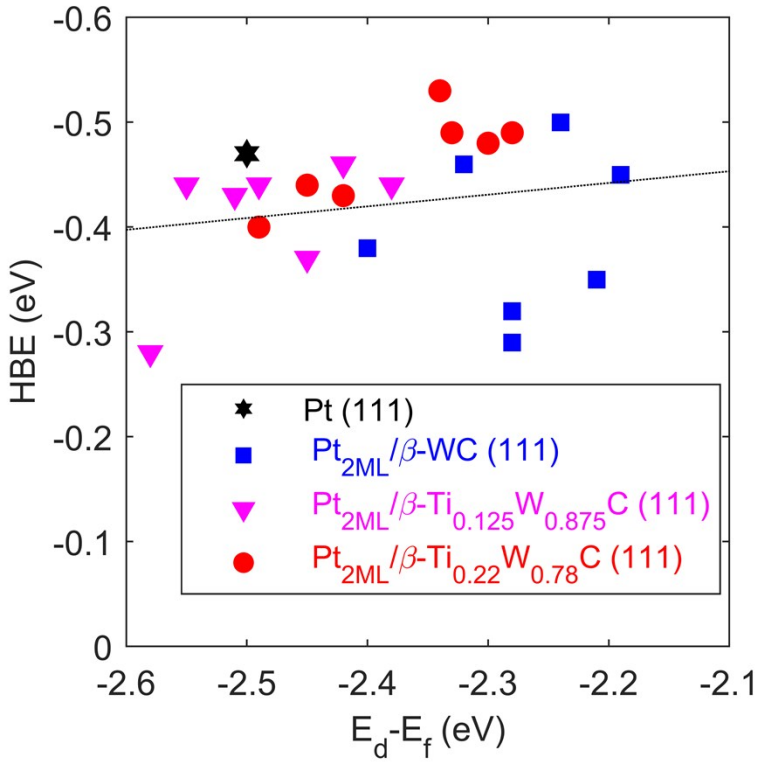

Figure S10. Hydrogen binding energy (HBE) versus *d*-band center relative to the Fermi-level (E_d-E_f) of various adsorption sites on Pt_{2ML}/β-$Ti_xW_{1-x}C$ (111) surfaces (Table S4); the solid line is a guide to the eye showing the approximate linear correlation

Table S1. Pt/WC slab models used in the calculation of formation energies; α and β are fixed at 90° for all slabs and θ is the relative rotation between the Pt (111) layer and the WC slab (see schematic in Figure S8)

	Slab Model	Wood's Notation	Relative rotation (θ)	Misfit factor (η)	Common unit cell
1.	$Pt_{1\text{-}2ML}$/α-WC (001)	p-(1x1) R0°	0°	+3.90%	a=2.92 Å, b=2.92 Å γ=120°
2.	$Pt_{1\text{-}2ML}$ /α-WC (001)	-	0°	+3.00%	a=2.92 Å, b=42.99 Å γ=109.84°
3.	$Pt_{1\text{-}2ML}$ /α-WC (001)	p-(4x4) R15°	15°	-0.10%	a=10.11 Å, b=10.11 Å γ=60°
4.	$Pt_{1\text{-}2ML}$ /β-WC (001)	-	4°	+1.05%	a=9.79 Å, b=19.58 Å γ=53.13°
5.	$Pt_{1\text{-}2ML}$ /β-WC (111)	p-(1x1) R0°	0°	+9.75%	a=3.10 Å, b=3.10 Å γ=120°
6.	$Pt_{1\text{-}2ML}$ /β-WC (111)	p-(4x4) R23.3°	23.3°	+1.19%	a=12.38 Å, b=12.38 Å γ=60°
7.	$Pt_{1\text{-}2ML}$ /β-WC (111)	-	23.3°	-1.38%	a=12.36 Å, b=24.52 Å γ = 19.11°
8.	$Pt_{1\text{-}2ML}$ /β-$Ti_xW_{1\text{-}x}C$ (111)	-	23.3°	-1.38%	a=12.36 Å, b=24.52 Å γ = 19.11°

Table S2. HBEs of β-$Ti_xW_{1-x}C$ (111) and Pt_{ML}/β-$Ti_xW_{1-x}C$ (111) surfaces with random and segregated substitution of W atoms with Ti atoms

Surface	**HBE (eV)**	
	Random	*Segregated*
β-$Ti_{0.125}W_{0.875}C$ (111)	-0.70	-0.65
β-$Ti_{0.22}W_{0.78}C$ (111)	-0.68	-0.65
Pt_{ML}/β-$Ti_{0.125}W_{0.875}C$ (111)	+0.03	-0.01
Pt_{ML}/β-$Ti_{0.22}W_{0.78}C$ (111)	+0.01	+0.03

Table S3. HBEs of various surfaces studied in this paper; the Pt layers can show significant heterogeneity in local strains and only the most stable binding energies among several sites sampled are reported here

Surface	Site	HBE (eV)
Pt (111)	Hcp hollow	-0.47
	Fcc hollow	-0.41
	Top	-0.42
α-WC (001)	Hcp hollow	-0.75
	Fcc hollow	-0.91
	Top	+0.38
Pt_{ML}/α-WC (001)	Hcp hollow	-0.41
	Fcc hollow	-0.38
	Top	-0.49
Pt_{2ML}/α-WC (001)	Hcp hollow	-0.52
	Fcc hollow	-0.52
	Top	-0.09
β-WC (001)	Bridge	-0.04
	Top W	+0.10
	Top C	-0.02
β-WC (111)	Hcp hollow	-0.94
	Fcc hollow	-0.94
	Top	-0.81
Pt_{ML}/ β-WC (111)	Hollow	-0.03
	Bridge	+0.01
	Top	+0.15
Pt_{2ML}/ β-WC (111)	Hollow	-0.50
	Bridge	-0.35
	Top	-0.45
β-$Ti_{0.125}W_{0.875}C$ (111)	Hcp hollow	-0.70
	Fcc hollow	-0.68
	Top	-0.60
Pt_{ML}/ β-$Ti_{0.125}W_{0.875}C$ (111)	Hollow	+0.06
	Bridge	+0.03
	Top	+0.16
Pt_{2ML}/ β-$Ti_{0.125}W_{0.875}C$ (111)	Hollow	-0.44
	Bridge	-0.46
	Top	-0.44
β-$Ti_{0.22}W_{0.78}C$ (111)	Hcp hollow	-0.68
	Fcc hollow	-0.64
	Top	-0.66
Pt_{ML}/ β-$Ti_{0.22}W_{0.78}C$ (111)	Hollow	+0.05
	Bridge	+0.01
	Top	+0.15
Pt_{2ML}/ β-$Ti_{0.22}W_{0.78}C$ (111)	Hollow	-0.53

	Bridge	-0.48
	Top	-0.49

Table S4. HBEs of various adsorption sites on $Pt_{2ML}/\beta\text{-}Ti_xW_{1-x}C$ (111) systems. Adsorption sites (top, bridge, and hollow) on $Pt_{2ML}/\beta\text{-}Ti_xW_{1-x}C$ surfaces are chosen based on the site-projected *d*-band center energy, E_d (relative to the Fermi level, E_f) to allow for systematic sampling of a range of HBEs. For bridge and hollow sites, the site-projected *d*-band energy is simply taken to be the average of the atom-projected *d*-band center energies of the nearest-neighbor Pt atoms.

Pt_{2ML}/β-WC (111)		
Adsorption Site	**E_d-E_f (eV)**	**HBE (eV)**
Top	-2.19	-0.45
Top	-2.40	-0.38
Bridge	-2.21	-0.35
Bridge	-2.28	-0.32
Hollow	-2.32	-0.46
Hollow	-2.24	-0.50
Hollow	-2.28	-0.29
$Pt_{2ML}/\beta\text{-}Ti_{0.125}W_{0.875}C$ (111)		
Adsorption Site	**E_d-E_f (eV)**	**HBE (eV)**
Top	-2.58	-0.28
Top	-2.38	-0.44
Bridge	-2.55	-0.44
Bridge	-2.42	-0.46
Hollow	-2.51	-0.43
Hollow	-2.45	-0.37
Hollow	-2.49	-0.44
$Pt_{2ML}/\beta\text{-}Ti_{0.22}W_{0.78}C$ (111)		
Adsorption Site	**E_d-E_f (eV)**	**HBE (eV)**
Top	-2.49	-0.40
Top	-2.28	-0.49
Bridge	-2.45	-0.44
Bridge	-2.30	-0.48
Hollow	-2.42	-0.43

Hollow	-2.33	-0.49
Hollow	-2.34	-0.53

References

1. J. E. Northrup and S. Froyen, *Phys. Rev. Lett.*, 1993, 71, 2276–2279.
2. J. E. Northrup and J. Neugebauer, *Phys. Rev. B*, 1995, 52, 17001–17004.
3. Y. Li, Y. Gao, B. Xiao, T. Min, Z. Fan, S. Ma and D. Yi, *Comput. Mater. Sci.*, 2011, **50**, 939–948.
4. J. L. R. Yates, G. H. Spikes and G. Jones, *Phys. Chem. Chem. Phys.*, 2015, **17**, 4250–4258.